Phytochemistry 91 (2013) 122–127

Contents lists available at SciVerse ScienceDirect

Phytochemistry

journal homepage: www.elsevier.com/locate/phytochem

Functional characterization of amyrin synthase involved in ursolic acid biosynthesis in *Catharanthus roseus* leaf epidermis

Fang Yu [a], Antje M.K. Thamm [a], Darwin Reed [b], Nemesio Villa-Ruano [a,c], Alfonso Lara Quesada [a,d], Edmundo Lozoya Gloria [e], Patrick Covello [b], Vincenzo De Luca [a,*]

[a] Department of Biological Sciences, Brock University, 500 Glenridge Avenue St. Catharines, ON, Canada L2S 3A1
[b] Plant Biotechnology Institute, Saskatoon, Saskatchewan, Canada S7N OW9
[c] Universidad de la Sierra Sur. Guillermo Rojas Mijangos S/N, Ciudad Universitaria, Miahuatlán de Porfirio Díaz, Oaxaca, CP 70800, Mexico
[d] Michael Smith Laboratories, University of British Columbia, 383 – 2185 East Mall Vancouver, B.C., Canada V6T 1Z4
[e] Genetic Engineering Department, Cinvestav Campus Guanajuato, Irapuato, Guanajuato, Mexico

ARTICLE INFO

Article history:
Available online 30 May 2012

Dedicated to the memory of Meinhart H. Zenk

Keywords:
Catharanthus amyrin synthase
Leaf epidermis expression
Ursolic acid
Secretion

ABSTRACT

Catharanthus roseus accumulates high levels of the pentacyclic triterpene, ursolic acid, as a component of its wax exudate on the leaf surface. Bioinformatic analyses of transcripts derived from the leaf epidermis provide evidence for the specialized role of this tissue in the biosynthesis of ursolic acid. Cloning and functional expression in yeast of a triterpene synthase derived from this tissue showed it to be predominantly an α-amyrin synthase (*CrAS*), since the α-amyrin to β-amyrin reaction products accumulated in a 5:1 ratio. Expression analysis of *CrAS* showed that triterpene biosynthesis occurs predominantly in the youngest leaf tissues and in the earliest stages of seedling development. Further studies using laser capture microdissection to harvest RNA from epidermis, mesophyll, idioblasts, laticifers and vasculature of leaves showed the leaf epidermis to be the preferred sites of *CrAS* expression and provide conclusive evidence for the involvement of this tissue in the biosynthesis of ursolic acid in *C. roseus*.

1. Introduction

The Madagascar periwinkle (*Catharanthus roseus*) is well known as the only commercial source of the anticancer dimeric monoterpenoid indole alkaloids (MIAs), vinblastine and vincristine, that have been used as chemotherapy agents since the 1970s. While this plant accumulates low levels of these dimers, they do accumulate more significant amounts of their precursor monomers, catharanthine and vindoline. Recent studies have provided extensive evidence that the assembly of MIAs in *Catharanthus* takes place in separate cell types. The Internal Phloem Associated Parenchyma (IPAP) cells appear to assemble part of the monoterpene skeleton (10-hydroxygeraniol; Burlat et al., 2004) and an undetermined intermediate appears to be transported by an unknown mechanism to the leaf epidermis, where at least the last two steps in this pathway are expressed to assemble secologanin (Irmler et al., 2000; Murata et al., 2008). The leaf epidermis-localized tryptophan decarboxylase also converts L-tryptophan into tryptamine that is combined with secologanin through the enzyme, strictosidine synthase to form strictosidine. The central intermediate of MIA biosynthesis (St-Pierre et al., 1999) can then be converted to several hundred MIAs found in *Catharanthus* (van Der Heijden et al., 2004) and to several thousand MIAs characterized in many other plant species (Szabo, 2008). Random sequencing of a cDNA library derived from *Catharanthus* leaf epidermis enriched RNA provided strong evidence that most of MIA pathway genes were preferentially expressed in this tissue (Murata et al., 2008). Additional studies have now established that while biosynthesis of catharanthine and vindoline occurs in young developing leaves, catharanthine accumulates in leaf wax exudates, while vindoline is found within the leaf. This is explained in part by the localization of the terminal reactions in vindoline biosynthesis to leaf mesophyll idioblasts and laticifers (Roepke et al., 2010). The spatial separations of vindoline from catharanthine explain why *Catharanthus* accumulates such low levels of dimeric anticancer drugs.

The thousands of biologically active triterpenes found in plants are derived from (3*S*)-oxidosqualene (**2**) (see Figs. 1 and 2) to generate over 80 different carbon skeletons (Ebizuka et al., 2003) via the activity of different oxidosqualene cyclase (OSC) enzymes that carry out the carbocation rearrangements responsible for this biological diversity. For example, *C. roseus* accumulates 2.5% of their leaf dry weights as the α-amyrin-derived ursane-type triterpene,

* Corresponding author. Tel.: +1 905 688 5550.
E-mail addresses: fyu@brocku.ca (F. Yu), at07ty@badger.ac.brocku.ca (A.M.K. Thamm), Darwin.reed@nrc-cnrc.gc.ca (D. Reed), nvilla@unsis.edu.mx (N. Villa-Ruano), alfonsol@msl.ubc.ca (A.L. Quesada), elozoya@ira.cinvestav.mx (E.L. Gloria), Patrick.covello@nrc-cnrc.gc.ca (P. Covello), vdeluca@brocku.ca (V. De Luca).

0031-9422/$ - see front matter © 2012 Elsevier Ltd. All rights reserved.
http://dx.doi.org/10.1016/j.phytochem.2012.05.002

ursolic acid (**4**) (Usia et al., 2005). Sequencing of the leaf epidermis-enriched transcripts also identified genes encoding enzymes of the mevalonic acid pathway (Fig. 1), as well as a new OSC gene with high amino acid sequence identity to amyrin synthases described in other plant species. Metabolite analysis showed that ursolic acid (**4**) was also secreted exclusively to the cuticular wax layer (Murata et al., 2008). Interestingly, two steps (PMK and MVD) in the MVA pathway were localized to the peroxisomes (Fig. 1) of *Catharanthus* (Simkin et al., 2011), confirming previous suggestions for compartmentation of this pathway in Arabidopsis (Sapir-Mir et al., 2008) and mammalian cells (Kovacs et al., 2007). The present study describes the functional expression of the *C. roseus* amyrin synthase (*CrAS*) in *Saccharomyces cerevisiae* and documents the highly regulated leaf epidermis specific expression of this gene during plant growth and development.

2. Experimental

2.1. Cultivation of C. roseus

The *C. roseus* (L.) G. Don, Little Delicata plants used in this study were cultivated in the greenhouse (Photoperiod 16 h:8 h/ light:-dark at 30 °C). For seedling developmental, studies *Catharanthus* seeds were immersed in EtoH–H_2O (7:3, v/v) for 1 min, and then thoroughly rinsed with sterile distilled H_2O for two times. After sterilization, seeds were incubated in H_2O in darkness for 24 h. After rinsing again with sterile distilled H_2O, 20–30 seeds per Petri dish were plated on wet filter papers and the dishes were transferred to the greenhouse (Photoperiod 16 h:8 h/light:dark at 30 °C) for cultivation for up to 12 days. Aliquots of 20 seedlings were harvested daily for gene expression analysis.

2.2. Isolation and cloning of C. roseus amyrin synthase

Young leaves from the 1st leaf pair (1 g) were harvested, immediately placed in liquid N_2, and ground thoroughly with a mortar and pestle. Total RNA extracted using TRIzol reagent (Invitrogen) was converted to cDNA by reaction with AMV Reverse Transcriptase (Promega) following standard protocols (Murata et al., 2005) to generate cDNAs used directly as PCR templates. A degenerate sense primer (5′-ATGTGGA**R**GCT**R**AAG**R**T**W**GC-3′, **R** = G or A, **W** = A or T) was designed according to the highly conserved 5′-end amino acid regions of known amyrin synthases. The anti-sense primer (5′-CTACAAGAAAACTTCTTGGATTTTTAC-3′) was designed according to known partial sequence from leaf epidermal-enriched cDNA library (Murata et al., 2008). PCR was carried out with *pfu* DNA polymerase (Fermentas) and the following cycling condition: 5 min at 95 °C (30 s at 95 °C, 30 s at 52 °C, 3 min at 72 °C) × 35 cycles. After gel purification and A-tailing using Taq DNA polymerase (Fermentas) of the PCR product, DNA of desired length was cloned into the pGEM-T easy vector (Promega) and transformed to XL-10 Gold Ultra-competent cells. The full-length sequence of

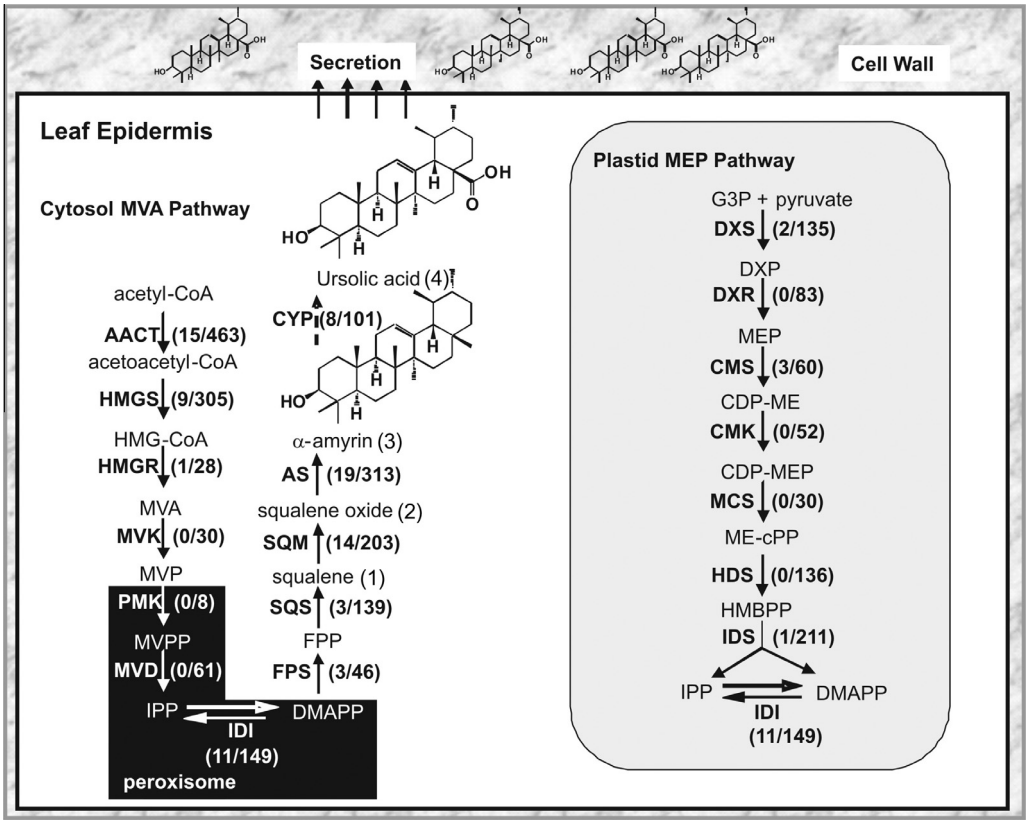

Fig. 1. The leaf epidermis is enriched in the mevalonic acid and ursolic acid pathways, but not in the 2-C-methyl-D-erythritol 4-phosphate/1-deoxy-D-xylulose 5-phosphate pathway (MEP/DOXP pathway). Bioinformatic analysis of a leaf epidermis enriched RNA sequence database (Murata et al., 2008) showed the frequency with which each gene encoding an enzyme in the mevalonic and ursolic acid biosynthetic pathways were expressed and this is compared with the frequency with which these genes were expressed in young whole *Catharanthus* leaves using a database containing 653,830 sequences obtained by 454 Pyrosequencing (Roche Diagnostics). The following abbreviations are used for different pathway enzymes: **AACT** (acetoacetyl CoA synthetase). **HMGS** (HMG CoA synthase); **HMGR** (HMG-CoA reductase); **MVK** (mevalonate kinase), **PMK** (phosphomevalonate kinase), **MVD** (mevalonate 5-pyrophosphate decarboxylase); **IDI** (isopenenyl pyrophosphate isomerase) **FPS** (farnesyl pyrophosphate synthase); **SQS** (squalene synthase); **SQM** (squalene monooxygenase); **AS** (αamyrin synthase); **DXS** (1-deoxy-D-xylulose 5-phosphate synthase); **DXR** (1-deoxy-d-xylulose 5-phosphate reductoisomerase); **CMS** (4-diphosphocytidyl-2-C-methyl-D-erythritol synthase); CMK (4-diphosphocytidyl-2-C-methyl-D-erythritol kinase); **MCS** (2-C-methyl-D-erythritol 2,4-cyclodiphosphate synthase); **HDS** (4-hydroxy-3-methylbut-2-en-1-yl diphosphate synthase) **IDS** (HMB-PP reductase).

Catharanthus amyrin synthase (*CrAs*) was obtained after sequencing of the plasmid DNA.

2.3. Functional expression of CrAS and product analyses in S. cerevisiae

The full-length coding sequence of the *CrAS* was PCR amplified using sense primer (5′-TAT**GAGCT**CATGTGGAAGCTAAAGATAGC-3′) which contains a Sac1 restriction site and anti-sense primer (5′-ATA**GGATCC**CTACAAAGCTTTGGTTGGCC-′) which contains BamH1 restriction site. The PCR product was digested with Sac1/BamH1 and cloned into the Sac1/BamH1 sites of the yeast expression vector pSCW231 under control of *ADH1* promoter and *CYCI* terminator to create pSCW231-*CrAS*.

The yeast strain MKP-0 (*MATa canl-100 ade2-1 lys2-1 ura3-52 leu2-3, 112 his3-D200 trpl-D901*) was transformed with pSCW231, pDM067 which contains *Saponaria vaccaria* β-amyrin synthase (Meesapyodsuk et al., 2007) and pSCW231-*CrAS* by the lithium acetate method, and transformants were selected on SD medium minus tryptophan (SD/-Trp). The recombinant yeast cells grew on 50 ml liquid SD/-Trp medium at 28 °C until stationary phase. MKP-0 yeast containing pSCW231 and pDM067 were used as controls.

For analysis of yeast products, the cells were harvested by centrifugation at 5000*g* for 10 min, and then saponified with 20% KOH in MeOH (2 ml) at 80 °C for 1 h. After extraction with hexane (2 ml) and water (2 ml), the hexane phase was dried and the residue was dissolved in BSA (Aldrich)/pyridine (1:1, 100 μl). An internal standard of cholesterol (10 μg) in CH_2Cl_2 (100 μl) dissolved in BSTFA/TMCS/pyridine (45:5:50, 20 μl) (Sigma) was added to the sample residue for analysis. GC–MS analysis was carried out as described in Meesapyodsuk et al. (2007), except that the temperature program was from 225 to 325 °C at 5 °C per min. A standard mixture of cholesterol, α-amyrin (**3**) and β-amyrin (**5**) (1:1:1) (Sigma) was used for response factor calibration. Mass spectral fragmentation data (GC–MS(EI) 70 eV) showed that the two peaks of interest produced in yeast expressing *C. amyrin* synthase had similar fragmentation patterns and were identical to the fragmentation patterns seen for reference standards of trimethylsilyl β-amyrin (*m/z* 218 [100], 203 [40], 73 [20] 189 [17], 95 [12], 135 [8], 55 [7], 279 [4], 498 $[M]^+$ [3], 257 [3], 393 [2], 483 $[M-CH_3]^+$ [1]) and trimethylsilyl α-amyrin (*m/z* 218 [100], 203 [17], 73 [23] 189 [23], 95 [13], 135 [13], 55 [8], 279 [6], 498 $[M]^+$ [4], 257 [2], 393 [2], 483 $[M-CH_3]^+$ [1]).

2.4. Extraction and analysis of triterpenes from Catharanthus leaves

Fresh individual leaf pairs representing different ages and developmental stages of growth were harvested and placed in $CHCl_3$ (5 ml) for 1 h in order to harvest leaf surface triterpenes and $CHCl_3$ extracts were dried by vacuum centrifugation in a SPD SpeedVac (Fisher Scientific) dryer. The $CHCl_3$ stripped leaves were air-dried in a fume hood for 60 min, pulverized with a mortar and pestle in the presence of N_2 and the powder was extracted with MeOH (5 ml) using a homogenizer. The extracts were centrifuged and the collected supernatant that was dried by vacuum centrifugation. The dried $CHCl_3$ and MeOH extracts were dissolved in MeOH (200 μl), filtered through a PALL filter (0.22 μm; VWR Canada) and analyzed by Ultra Performance Liquid Chromatography–Mass Spectroscopy (UPLC–MS) using an Acquity™ C18 column with particle size of 1.7 mm and column dimensions of 1.0 × 50 mm. The solvent systems to resolve triterpenes used A (H_2O) and B (CH_3CN) to form a linear gradient using the following conditions: 0–0.6 min 99% A, 1% B at 0.3 mL/min, 0.6–5 min 99% A and 1% B at 0.4 mL/min, 5–8 min gradient to 1% A and 99% B at 0.4 mL/min, 8.00–8.50 min gradient to 99% A and 1% B at 0.4 mL/min and 8.50–10 min 99% A and 1% B at 0.3 mL/min (Murata et al., 2008).

2.5. Sequence alignment and phylogenetic analysis

The protein sequence of *CrAS* (GenBank JQ027033) was aligned with 47 full-length functionally characterized amyrin synthases from other plant species using ClustalW 2 (www.align.genome.jp/). The predicted *CrAS* amino acid sequence was submitted to DNA distance neighbor-joining phylogenetic analysis using BioEdit (www.mbio.ncsu.edu/BioEdit/bioedit.html) and visualized with Phylodraw (www.pearl.cs.pusan.ac.kr/phylodraw/).

3. Results and discussion

3.1. Phylogenetic analysis associates C. roseus amyrin synthase (CrAS) with known α/β amyrin synthases

A single candidate amyrin synthase gene encoding an incomplete open reading frame appeared to be represented 19 times (Fig. 1) within the *Catharanthus* leaf epidermis enriched library (Murata et al., 2008). The full length clone (*CrAS*) obtained as described in the Section 2 was submitted to phylogenetic analysis with 47 putative (some functionally characterized) amyrin synthases (Supplementary Fig. S1). The 762 amino acid open reading frame of *CrAS* showed 86% amino acid sequence identity (Supplementary Figs. S1 and S2) to a 763 amino acid mixed function oxidosqualene cyclase (OEA) from olive (*Olea europaea*) which produced a mixture of α- (**3**) and β-amyrin (**5**) (Fig. 2), as well as small amounts of ψ-taraxasterol and butyrospermol when expressed in yeast (Saimaru et al., 2007). In contrast, *CrAS* showed only 60% amino acid sequence identity (Supplementary Figs. S1 and S2) to a 760 amino acid *S. vaccaria* β-amyrin synthase (SvBS) that produces β-amyrin (**5**) exclusively when expressed in yeast (Fig. 2) (Meesapyodsuk et al., 2007). The results provided clues that *CrAS* might in fact be the α-amyrin synthase (Fig. 2) involved in production of the direct precursor of ursolic acid (**4**) that accumulates on the surface of *Catharanthus* leaves ((Murata et al., 2008). *CrAS* also contains the amino acid motif DCTAE, thought to form part of the active site that binds oxidosqualene (**2**) (Abe et al., 1995), a number of QW motifs shown to be shared by the OSC superfamily (Poralla et al., 1994) and the MWCYCR motif that specifies the formation of *β*-amyrin (**5**) in *Panax ginseng* (Kushiro et al., 2000).

3.2. CrAS possesses α-amyrin synthase activity when expressed in yeast

Functional expression of *CrAS* produced a yeast strain that accumulated α-amyrin (**3**) as a major product (Fig. 3a), as well as small amounts of β-amyrin (**5**) when compared to the control strain that does not accumulate either triterpene (Fig. 3b) or to yeast expressing SvBS that only accumulates small amounts of these two products (Fig. 3c). When three biological replicates were analyzed (Fig 3 inset), the *CrAS* line accumulated up to 5 times more α-amyrin (**3**) (103 ± 19 μg) than the β- (**5**) (21.9 ± 4 μg) form and together this line accumulated up to 14 times more totalamyrins than β-amyrin (**5**) (8.6 ± 1.5 μg) accumulating in the SvBS line. This preferred production of α-amyrin (**3**) by *CrAS* was also observed when apple *MdOSC1* (Brendolise et al., 2011) was expressed in the yeast, *Pichia methanolica*. Inspection of the apple α/β-amyrin synthase amino acid sequences (MDOSC1 & 3) suggests that they resemble the multifunctional triterpene synthase *KcMS*, and the lupeol synthase *BgLUS*, while they are not closely related to *CrAS*, showing only 54% amino acid sequence identity over 758 amino acids (Supplementary Fig. 1). Amino acid sequence comparisons conducted with

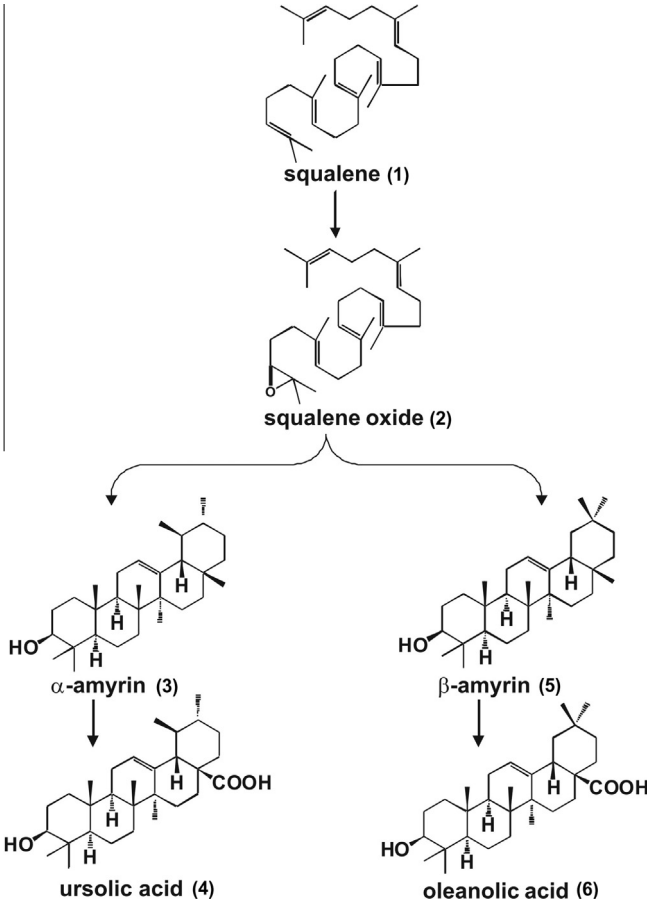

Fig. 2. Biosynthesis of ursolic (**4**) and oleanolic acids (**6**) from squalene oxide (**2**). Multifunctional amyrin synthases expressed in recombinant yeast have been shown to convert the common precursor, squalene oxide via a lupanyl cation to the cyclization products α- and β-amyrin (**3** and **5**). Various amyrin synthases produce these products in different ratios that may representative of the ursane and/or oleanane skeletons found in the parent plant species.

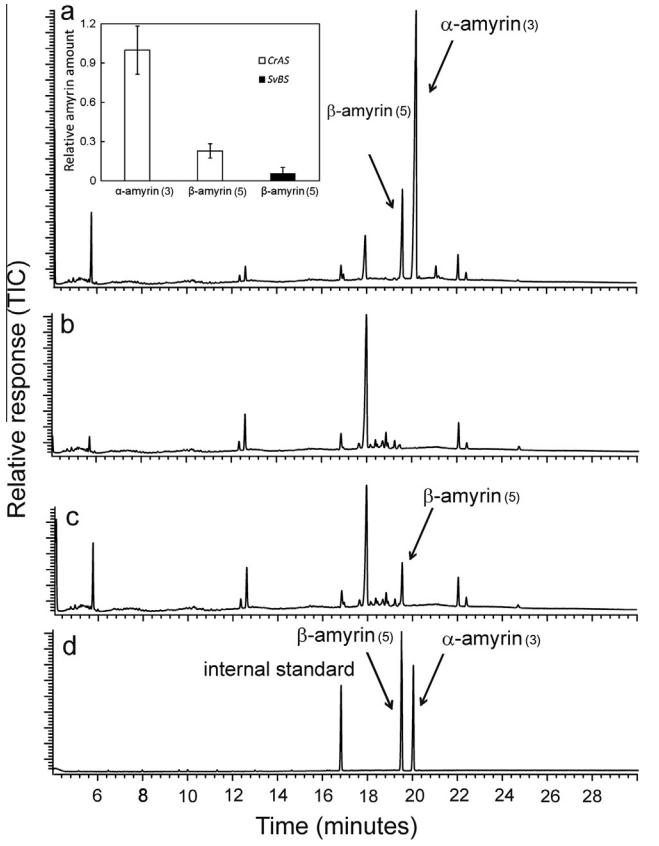

Fig. 3. Analysis by GC–MS of the relative accumulation of α- and β-amyrin (**3**) and (**5**) produced in *S. cerevisiae* strains expressing recombinant *CrAS* and SvBS. Total ion chromatograms are shown for extracts of yeast strains (a) expressing *CrAS*; (b) without *CrAS* expression; (c) expressing SvBS; (d) α- and β-amyrin (**3** and **5**) standards together with the internal cholesterol standard. Inset: ratio of β-amyrin to α-amyrin accumulating in *CrAS*- (white bars) and SvBS-expressing yeast strains (black bars). The error bars represent standard errors from three biological replicates.

apple MdOSC1 were used to suggest that substitution of F for W in the ^{256}MFCYCR^{261} motif might be partly responsible for the increased α-amyrin (**3**) product specificity observed (Brendolise et al., 2011). However the presence of W in the ^{256}MWCYCR^{261} motif of *CrAS* suggests that creation of α-amyrin (**3**) product specificity involves changes at other amino acid positions. The similar biochemical properties of *CrAS* and MdOSC1 also show that evolution of α-amyrin (**3**) product specificity could have occurred more than once after divergence of this multifunctional triterpene synthase family.

3.3. *CrAS is preferentially expressed in leaf epidermis, in younger leaves and during the earlier stages of seedling development in C. roseus*

RNA obtained from the epidermis, mesophyll, idioblast, laticifer and vasculature of leaves by laser capture microdissection was converted to cDNA (Murata and De Luca, 2005; Murata et al., 2006) and each tissue type was probed for expression of *CrAS*. While whole leaves and leaf epidermis were the preferred sites of *CrAS* expression (Fig 4a), the mesophyll, idioblast, laticifer and vasculature cells were not. In contrast, actin was expressed to similar levels in all cell types studied. These results corroborate earlier studies suggesting that the leaf epidermis is enriched in the mevalonic acid and ursolic acid pathways (Murata et al., 2008).

Leaves of different ages were extracted for total RNA (Murata et al., 2005) and the expression profile of *CrAS* with age was determined by real time RT-PCR. The results showed that the youngest leaves appear to be most active in ursolic acid (**4**) biosynthesis and this activity declined with leaf age (Fig. 4b). The expression profile of *CrAS* also corresponded closely with the accumulation profile of ursolic acid (**4**) on the leaf surfaces where maximum levels were achieved in leaf pair 3 and beyond with levels varying between 0.7 and 1 mg/leaf pair (Fig. 4c). When ursolic acid (**4**) levels per cm^2 of leaf surface in leaves of different ages were compared, the highest levels were found in the youngest leaves and they were diminished rapidly with leaf age and leaf expansion, reflecting the importance of very young tissues in the biosynthesis and secretion of this triterpene in *C. roseus* (Fig. 4d). Together these data suggest that ursolic acid (**4**) biosynthesis and accumulation follow a very similar developmental program to that of MIA biosynthesis (Murata et al., 2008).

The co-expression of MIA, flavonoid, triterpenoid and very-long chain fatty acid (VLFA) biosynthesis pathways within the leaf epidermome of *C. roseus* was a highlight of this previous study (Murata et al., 2008). This remarkable organization of the epidermome during the early stages of leaf development to accommodate several metabolic pathways represents a unique opportunity to study the components of cellular specialization that may be important for making different types of special metabolites within the same cells (Mahroug et al., 2006). These processes are coupled to largely

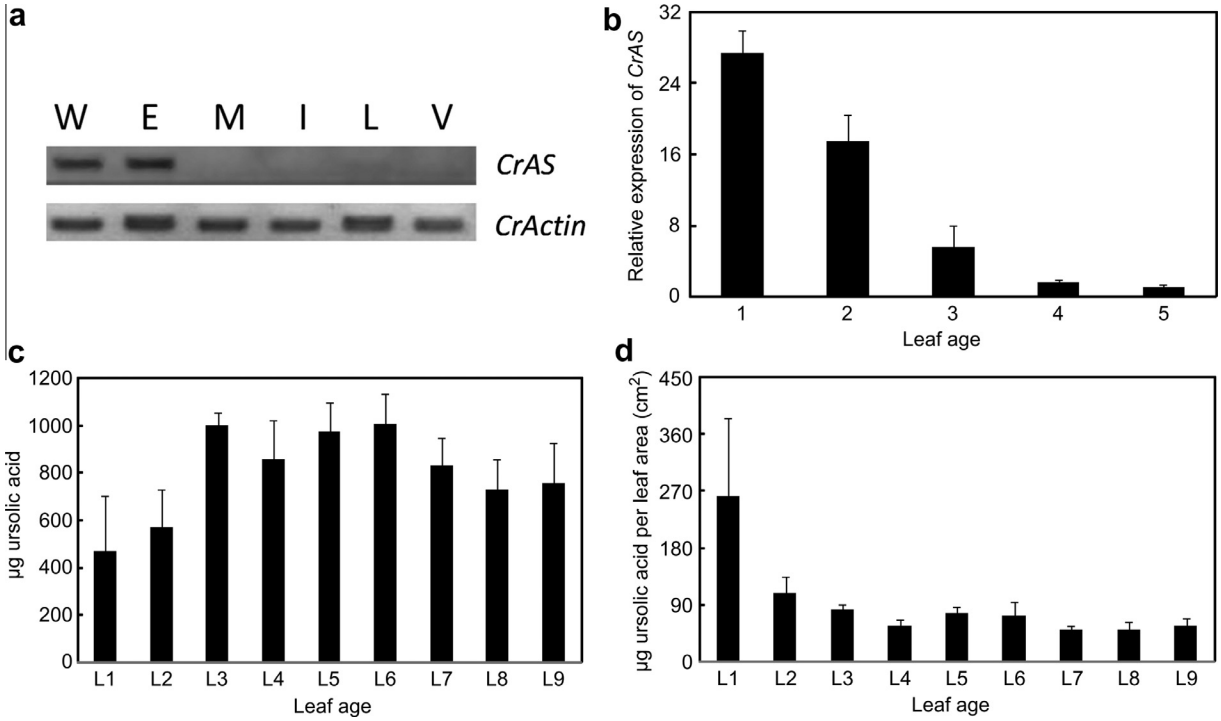

Fig. 4. Preferential expression of *CrAS* in *Catharanthus* leaf epidermis, in younger leaf tissues and in younger stages of seedling development is correlated with the timing ursolic acid accumulation of the leaf surface. (a) Laser capture microdissection was used to harvest whole leaves (W), leaf epidermis (E), leaf mesophyll (M), leaf idioblast (I), laticifer (L) and leaf vasculature (V) cells for RNA isolation and for performing RT-PCR using probes for *CrAs* and *CrActin*. (b) Quantitative RT PCR analysis of expression levels of *CrAS* was performed with extracts from leaves of different developmental ages (leaf pairs 1, 2, 3, 4 and 5). (c) Accumulation of ursolic acid (**4**) (µg/leaf pair) in leaves of different ages (leaf pairs 1, 2, 3, 4, 5, 6, 7, 8 and 9). (d) Accumulation of ursolic acid (µg/cm^2 of leaf surface) in leaves of different ages (leaf pairs 1, 2, 3, 4, 5, 6, 7, 8 and 9). The error bars in (b), (c) and (d) represent standard errors from three biological replicates.

non-characterized secretory mechanisms that permit the export of VLSAs, triterpenes and MIAs (catharanthine) (Roepke et al., 2010) to the leaf surface. The accumulation of VLFAs, triterpenes and MIAs on the leaf surface may provide general protection to the plant from various diseases and insects, as well as providing a barrier against water and nutrient loss.

The preferential expression of *CrAS* in young *Catharanthus* leaves prompted investigations to determine when this gene would be expressed during seedling germination and development (Fig. 5). Analyses of whole seedlings showed that triterpene biosynthesis is activated at very early stages of germination with relative expression of *CrAS* at day 1 being 7 times higher than at day 12 and this expression increased until day 5, after which transcript levels decreased continually (Fig. 5). The early expression of triterpene biosynthesis is in contrast to MIA biosynthesis that appears to peak over a period of 72 to 96 h from day 4 to day 7 of seedling development (De Luca, 2011). These results provide novel insights concerning the possible timing differences between triterpene and MIA biosynthesis that might be further investigated using developing seedlings as a model system.

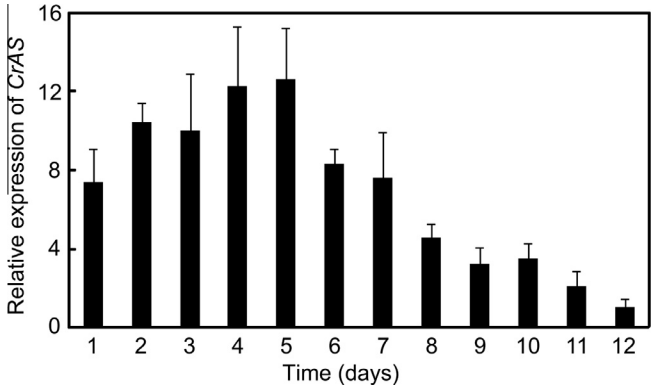

Fig. 5. Expression of *CrAS* during seed germination and seedling development. Quantitative RT PCR analysis of expression levels of *CrAS* was performed with extracts of seedlings from day 1 to 12 of development. The error bars represent standard errors from three biological replicates.

4. Conclusions

C. roseus accumulates up to 2.5% of its dry weight as the ursane type triterpene, ursolic acid (**4**) (Usia et al., 2005) as a component of the wax exudates on the leaf surface (Murata et al., 2008). Remarkably, catharanthine, a major MIA of *Catharanthus* also accumulates almost exclusively in this wax exudate (Roepke et al., 2010). The present study provides chemical, biochemical and molecular evidence that biosynthesis of ursolic takes place in the leaf epidermis by confirming the α-amyrin synthase activity of recombinant *CrAS*. The developmental regulation of this gene is described during seedling development and its preferred expression in younger leaves and in the leaf epidermis rather than in other tissue types is shown by laser capture microdissection (Murata and De Luca, 2005).

Acknowledgements

This work was supported through funding provided by the Natural Sciences and Engineering Research Council of Canada in the form of a Discovery Grant and a Research Tools and Infrastructure Grant, by Genome Canada and by the Canada Foundation for Innovation – Leaders Opportunity Fund. VDL holds a Tier 1 Canada Research Chair in Plant Biochemistry and Biotechnology.

Research Council of Canada (NSERC) to V.D.L. V.D.L. holds a Canada Research Chair in Plant Biotechnology. N.V.R. thanks the

Mexican government for funds to spend 4 months in the laboratory of V.D.L.

Appendix A. Supplementary data

Supplementary data associated with this article can be found, in the online version, at http://dx.doi.org/10.1016/j.phytochem.2012.05.002.

References

Abe, I., Prestwich, G.D., 1995. Identification of the active site of vertebrate oxidosqualene cyclase. Lipids 30, 231–234.

Brendolise, C., Yauk, Y.K., Eberhard, E.D., Wang, M., Chagne, D., Andre, C., Greenwood, D.R., Beuning, L.L., 2011. An unusual plant triterpene synthase with predominant α-amyrin producing activity identified by characterising oxidosqualene cyclases from *Malus domestica*. FEBS J. 278, 99–2485.

Burlat, V., Oudin, A., Courtois, M., Rideau, M., St-Pierre, B., 2004. Co-expression of three MEP pathway genes and geraniol 10-hydroxylase in internal phloem parenchyma of *Catharanthus roseus* implicates multicellular translocation of intermediates during the biosynthesis of monoterpene indole alkaloids and isoprenoid-derived primary metabolites. Plant J. 38, 131–141.

De Luca, V., 2011. In: Crozier, A., Ashihara, H. (Eds.), Plant Metabolism and Biotechnology: Monoterpenoid Indole Alkaloid Biosynthesis. John Wiley and Sons, pp. 263–292.

Ebizuka, Y., Katsube, Y., Tsutsumi, T., Kushiro, T., Shibuya, M., 2003. Functional genomics approach to the study of triterpene biosynthesis. Pure Appl. Chem. 75, 369–374.

Irmler, S., Schroeder, G., St-Pierre, B., Crouch, N.P., Hotze, M., Schmidt, J., Strack, D., Matern, U., Schroeder, J., 2000. Indole alkaloid biosynthesis in *Catharanthus roseus*: New activities and identification of cytochrome P450 CYP72A1 as secologanin synthase. Plant J. 24, 797–804.

Kovacs, W.J., Tape, K.N., Shackelford, J.E., Duan, X., Kasumov, T., Kelleher, J.K., Brunengraber, H., Krisans, S.K., 2007. Localization of the presqualene segment of the isoprenoid biosynthetic pathway in mammalian peroxisomes. Histochem. Cell Biol. 127, 273–290.

Kushiro, T., Shibuya, M., Masuda, K., Ebizuka, Y., 2000. Mutational studies on triterpene synthases: engineering lupeol synthase into β-amyrin synthase. J. Am. Chem. Soc. 122, 6816–6824.

Mahroug, S., Courdavault, V., Thiersault, M., St-Pierre, B., Burlat, V., 2006. Epidermis is a pivotal site of at least four secondary metabolic pathways in *Catharanthus roseus* aerial organs. Planta 223, 1191–1200.

Meesapyodsuk, D., Balsevich, J., Reed, D.W., Covello, P.S., 2007. Saponin biosynthesis in *Saponaria vaccaria*. cDNAs encoding β-amyrin synthase and a triterpene carboxylic acid glucosyltransferase. Plant Physiol. 143, 959–969.

Murata, J., De Luca, V., 2005. Localization of tabersonine 16-hydroxylase and 16-OH tabersonine-16-*O*-methyltransferase to leaf epidermal cells defines them as a major site of precursor biosynthesis in the vindoline pathway in *Catharanthus roseus*. Plant J. 44, 581–594.

Murata, J., Bienzle, D., Brandle, J.E., Sensen, C.W., De Luca, V., 2006. Expressed sequence tags from Madagascar periwinkle (*Catharanthus roseus*). FEBS Lett. 580, 4501–4507.

Murata, J., Roepke, J., Gordon, H., De Luca, V., 2008. The leaf epidermome of *Catharanthus roseus* reveals its biochemical specialization. Plant Cell 20, 524–542.

Poralla, K., Hewelt, A., Prestwich, G.D., Abe, I., Reipen, I., Sprenger, G., 1994. A specific amino acid repeat in squalene and oxidosqualene cyclases. Trends Biochem. Sci. 19, 157–158.

Roepke, J., Salim, V., Wu, M., Thamm, A.M.K., Murata, J., Ploss, K., Boland, W., De Luca, V., 2010. Vinca drug components accumulate exclusively in leaf exudates of Madagascar periwinkle. PNAS 107, 15287–15292.

Saimaru, H., Orihara, Y., Tansakul, P., Kang, Y.H., Shibuya, M., Ebizuka, Y., 2007. Production of triterpene acids by cell suspension cultures of *Olea europaea*. Chem. Pharm. Bull. 55, 784–788.

Sapir-Mir, M., Mett, A., Belausov, E., Tal-Meshulam, S., Frydman, A., Gidoni, D., Eyal, Y., 2008. Peroxisomal localization of Arabidopsis isopentenyl diphosphate isomerases suggests that part of the plant isoprenoid mevalonic acid pathway is compartmentalized to peroxisomes. Plant Physiol. 148, 1219–1228.

Simkin, A.J., Guirimand, G., Papon, N., Courdavault, V., Thabet, I., Ginis, O., Bouzid, S., Giglioli-Guivarc'h, N., Clastre, M., 2011. Peroxisomal localisation of the final steps of the mevalonic acid pathway in planta. Planta 234, 903–914.

St-Pierre, B., Vazquez-Flota, F.A., De Luca, V., 1999. Multicellular compartmentation of *Catharanthus roseus* alkaloid biosynthesis predicts intercellular translocation of a pathway intermediate. Plant Cell 11, 887–900.

Szabo, L.F., 2008. Rigorous biogenetic network for a group of indole alkaloids derived from strictosidine. Molecules 13, 1875–1896.

Usia, T., Watabe, T., Kadota, S., Tezuka, Y., 2005. Cytochrome P450 2D6 (CYP2D6) inhibitory constituents of *Catharanthus roseus*. Biol. Pharm. Bull. 28, 1021–1024.

van Der Heijden, R., Jacobs, D.I., Snoeijer, W., Hallard, D., Verpoorte, R., 2004. The Catharanthus alkaloids: pharmacognosy and biotechnology. Curr. Med. Chem. 11, 607–628.